Genetically Designed Wire Bundle Superscatterers

Konstantin Grotov, Dmytro Vovchuk, Sergei Kosulnikov, Ilya Gorbenko, *Student Member, IEEE*, Leon Shaposhnikov, Konstantin Ladutenko, Pavel Belov, *Member, IEEE*, and Pavel Ginzburg, *Member, IEEE*

***Abstract*— Experimental demonstration of superdirectivity and superscattering phenomena is among the long-standing challenges in electromagnetic theory. Efficient computational algorithms can contribute to this endeavor by suggesting new designs bypassing commonly accepted limitations. Here, we demonstrate a rectangular wire bundle superscatterer designed using a stochastic optimization algorithm. The structure encompassing wires of different lengths demonstrates superior scattering capabilities, bypassing the single channel dipole limit by an order of magnitude. The subwavelength wire bundle supports several resonant higher-order multipoles, which constructively contribute to the scattering, as we demonstrate experimentally. A new generation of genetically designed superscatterers may be used in a range of wireless applications, including point-to-point communications, smart beacons, and radar targets.**

***Index Terms*— Genetic algorithm, scattering limit, superscattering, wire bundle.**

I. Introduction

THE maximization or suppression of electromagnetic scattering on subwavelength structures has always been subject to extensive investigations owing to fundamental challenges and promising applications. The objective of scattering enhancement is closely related to antenna applications [1], while the opposite goal is inspired by radar invisibility needs [2]–[4]. Since the vast majority of airborne objects interrogated by low-frequency surveillance radars [5] are seen by the latter as subwavelength, typical stealth high-frequency approaches are not applicable in this case.

Electromagnetic scattering on compact structures is well approximated by a multipole series, where lower orders are typically sufficient for convergence [6]. Maximal possible scattering into a single multipole is called a channel limit. In many cases, a dipole single channel limit (the maximal scattering cross section, which a small resonant lossless dipole can approach) is considered. In this case, $3\lambda^2/(2\pi)$, where λ is free space wavelength, the value used for all the assessments hereafter. Compact subwavelength structures bypassing the single channel limit are called superscatterers. While there is no fundamental upper bound on a scattering cross section, quite a few theoretical limits with Chu–Harrington [7], being the most used, have been proposed to account for possible practical aspects. Bypassing those limits requires accommodating several resonant multipoles, constructively interfering at nearly the same frequency. While there is no one-to-one correspondence between internal resonances of a structure and resonant multipoles forming the far-field scattering, it is quite evident that a superscatterer should employ a resonant phenomenon [8], [9]. In this case, a significant near-field accumulation in the vicinity of lossy materials accompanied by an extremely low fabrication tolerance is the main known factors limiting practical demonstration of superscatterers [10]. Nevertheless, several promising designs were demonstrated during the last years and will be revised hereinafter. Regardless of their realization, they all share the same design principles. The first one is the choice of a material platform. Since strong near-field accumulation necessarily implies high ohmic losses, constitutive components should be carefully chosen. In particular, copper wires and foam hosts are among the most promising candidates [9], [11]. The second criterion is the capability to perform extensive electromagnetic optimization. In the case of compact structures, internal resonances tend to repel each other, opening frequency gaps. To bypass these design challenges, optimization efforts are performed. Spherically or cylindrically symmetric architectures have an advantage owing to fast semi-analytical computation algorithms based on Mie solutions of the electromagnetic problem. However, investigation of structures with a high internal symmetry might overlook remarkable properties, which are granted by architectures with a broken symmetry. Those configurations can be obtained with genetic algorithms. Starting with a conventional geometry, optimization routines can evolve into shapes, which are hardly predictable.

Evolutionary algorithms, with a genetic optimization being a subset, have received special attention in electromagnetism.

Manuscript received 25 January 2022; revised 26 April 2022; accepted 3 May 2022. Date of publication 30 May 2022; date of current version 9 November 2022. The work of Dmytro Vovchuk, Pavel Ginzburg, and Sergei Kosulnikov was supported by the Department of the Navy, Office of Naval Research Global (ONRG), under Award N62909-21-1-2038. The work of Konstantin Grotov, Leon Shaposhnikov, Konstantin Ladutenko, Pavel Belov, and Sergei Kosulnikov, was supported in part by the Priority 2030 Federal Academic Leadership Program and in part by the Russian Science Foundation under Project 21-79-30038. The work of Ilya Gorbenko was supported in part by the Priority 2030 Federal Academic Leadership Program, in part by the Russian Science Foundation under Project 21-79-30038, and in part by the IEEE Microwave Theory and Techniques Society (MTT-S Undergraduate/Pre-graduate Scholarship (2021 Cycle 1 Awards)). *(Konstantin Grotov and Dmytro Vovchuk contributed equally to this work.) (Corresponding author: Dmytro Vovchuk.)*

Konstantin Grotov, Leon Shaposhnikov, Konstantin Ladutenko, and Pavel Belov are with the School of Physics and Engineering, ITMO University, 197101 Saint Petersburg, Russia (e-mail: konstantin.grotov@metalab.ifmo.ru).

Dmytro Vovchuk and Pavel Ginzburg are with the School of Electrical Engineering, Tel Aviv University, Tel Aviv 69978, Israel (e-mail: dimavovchuk@gmail.com; pginzburg@tauex.tau.ac.il).

Sergei Kosulnikov is with the School of Physics and Engineering, ITMO University, 197101 Saint Petersburg, Russia, and also with the Centre of Nanoheterostructure Physics, School of Physics, Tel Aviv University, Tel Aviv 69978, Israel (e-mail: s.y.kosulnikov@gmail.com).

Ilya Gorbenko is with the School of Physics and Engineering, ITMO University, 197101 Saint Petersburg, Russia, and also with the Ioffe Institute, 194021 Saint Petersburg, Russia.

This article has supplementary material provided by the authors and color versions of one or more figures available at https://doi.org/10.1109/TAP.2022.3177531.

Digital Object Identifier 10.1109/TAP.2022.3177531

The concept is to treat electromagnetic configuration as a basic provision in the theory of biological evolution, where processes of selection, mutation, and reproduction govern future development. Evolutionary algorithms [12] are widely used in multidimensional domains, where the functional dependence between parameters is either non-differentiable or has many local extrema. These algorithmic approaches were introduced into engineering problems in the 1960s [13], and since then, being supported by ever-growing computational power, started to shift aside conventional design rules. One of the most known electromagnetic examples is the NASA spacecraft antenna [14], which was designed from a paper pin and evolved into an efficient compact X-band antenna. In the field of the current paper, it is worth mentioning multilayer circular rod superscatterers [15], superabsorptive nanoparticles [16], core-shell cylindrical superscatterers [17], subwavelength superscattering nanospheres [18], design of optimized nanoplasmonic materials [19], antenna design [14], [20]–[24], photonic crystal design [25], antireflective coating for photovoltaics [26], nanoplasmonic particles [27], [28], new magnetic materials with high magnetization [29], and others [30]–[33].

Here, we design and experimentally demonstrate a new superscatterer architecture. Our structure is based on a wire bundle made from thin copper wires and a Styrofoam host. These constitutive elements, being an extremely low loss at GHz spectral range, can accommodate a significant near-field concentration without introducing severe ohmic losses. Furthermore, the structure based on metal wires can be efficiently solved using Hallen's and Pocklington's integral equations [34], which is a powerful tool for solving complex problems, i.e., including motion (e.g., [35], [36]).

The capability to obtain a fast-forward problem solution (electromagnetic scattering in our case) is the key for converging to a reliable solution granted by the evolutionary algorithm.

The manuscript is organized as follows. The stochastic optimization algorithm is introduced first and then followed by an electromagnetic analysis of its performance. Experimental demonstration of superscattering and discussion on superdirectivity aspects of the new structure come before the conclusion.

II. Optimization Algorithm

The wire bundle, being potentially a low-loss fabrication-tolerant geometry, was chosen as a starting point for the optimization. To reduce the search space, a 3×3 cubic array with vertically aligned equidistant wires was taken as a constraint, though it will be reconsidered later. The length of each individual wire is allowed to change independently, while the wire's radius is kept constant ($r = 0.5$ mm) to comply with the forthcoming experiment. Another constraint is the radius of an imaginary enclosing sphere, which is kept being less than 30 mm. This parameter is especially important for a future assessment of superscattering performances, as the structure should be kept subwavelength. The number of independent continuous parameters in the system is N^2 ($N = 3$), though there are symmetry considerations to apply. In particular, reflection symmetry with respect to the plane containing the k-vector of the linearly polarized incident wave and its electric field vector was imposed to obtain directive forward scattering. The field is polarized along the wires. The symmetry constraint will also be relaxed at later stages, and consequences will be discussed. The target function, subject to maximization, was taken to be the total scattering cross section of the system at 6 GHz central operational frequency.

Since the target function may have several local extrema, a stochastic optimization was used covariance matrix adaptation evolution strategy (CMA-ES) [37]. A fast-forward solver using Hallen integral formulation realized in python numerical electromagnetics code (PyNEC) was employed. The following parameters were fixed before running the optimization: population size, mutation strength, and a number of generations. A population size was $3N^2$ ($N = 3$), mutation strength was chosen as 20% of the corner wires length limit, which is the maximum amount by which the length of the wire changes after a mutation. Thus, during optimization, the radius of the described sphere around geometry, the distance between the wires, the number of wires, the population size, mutation strength, and a number of generations were fixed, and the length of each wire was optimized. The algorithm was terminated after 500 generations, which was revealed empirically for a sufficient convergence of structures with $N = 2$, 3, and 4. For $N = 3$ case, one generation took 0.22 s, and all 500 steps took 110 s. All calculations were carried out using Intel Xeon E3 1230 v6 3,5 GHz CPU and 64 GB of RAM. After optimization, the best structures were selected according to two criteria. First, the structure must be reproducible; i.e., it should be obtainable with different random initial parameters. Second, a random 2% change in the wires' lengths should not affect the total scattering by more than 10% (those thresholds were also identified empirically). Fig. 1 summarizes the main parameters and steps of the algorithm.

III. Multipolar Analysis of the Results

The algorithm generated several designs, which will be analyzed hereinafter. The modeling of the best-found designs was performed with CST Microwave Studio, a frequency-domain solver with the incident field linearly polarized along the wires [inset of Fig. 2(a)]. Since high-quality factor (Q-factor) modes are involved, a frequency domain analysis is preferred, as it provides more accurate and stable solutions. Two final geometries [Fig. 2(a) and (b)], which differ from each other quite significantly, were chosen for the analyses. Wires lengths in a form of 3×3 matrix appear in the Supplementary Material. Black solid lines in Fig. 2(c) and (d) correspond to the total scattering cross sections normalized to the single-channel limit. As it can be seen, both geometries demonstrate a strong scattering peak around 6 GHz, as it was designed. In terms of the performances, the single-channel limit was overcome by more than an order of magnitude. The second geometry though shows slightly better performances.

While the optimization algorithm ends up in a certain structure's realization, it does not provide any physical interpretation of its operating principles. The key assessment to be made here is to compare the scattering performance with a single-channel limit and verify that indeed several multipoles have a significant spectral overlap. Multipolar expansion to the total scattering cross section appears in Fig. 2(c) and (d).

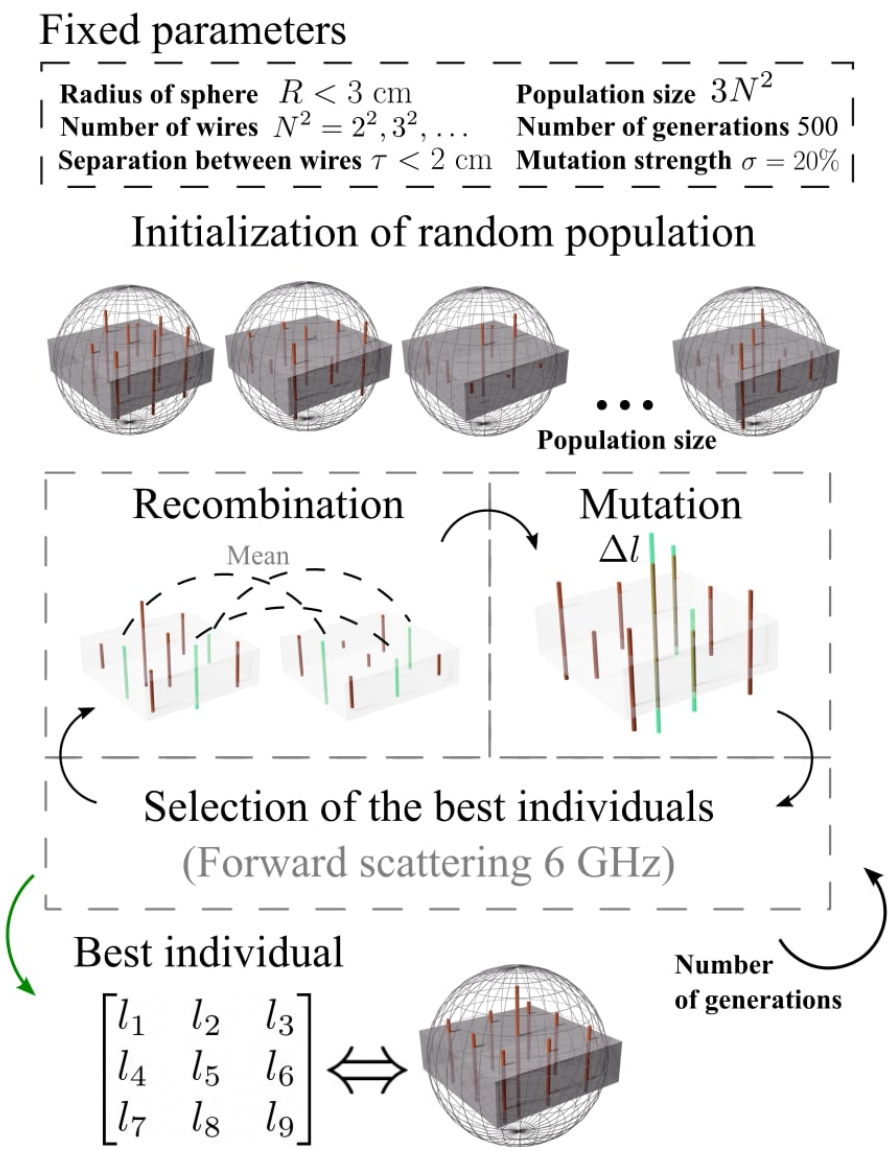

Fig. 1. Block diagram of the evolution strategy undertaken in the optimization algorithm. Gray rectangle contains fixed hyperparameters constraining the optimization. The black dashed rectangle unifies the algorithmic steps.

The following abbreviations are used: electric dipole (ED), magnetic dipole (MD), electric quadrupole (EQ), magnetic quadrupole (MQ), electric octupole (EO), and magnetic octupole (MO). Since the multipole series converge to the total scattering cross section quite well (black solid versus black dashed line), higher-order multipoles can be ignored. In both realizations, several multipoles resonate at the same frequency. Geometry A [Fig. 2(a)] mainly relies on two major resonances, while the second realization [Fig. 2(b)] demonstrates three spectrally co-located multipoles. Nevertheless, the performances of those conceptually different realizations are quite similar. It is also worth noting that the dipole contributions here are rather negligible, while higher-order poles provide the major effect. This is one of the reasons why the dipole single-channel limit here is significantly surpassed. Far-field directivity patterns appear as insets in Fig. 2(c) and (d), demonstrating a strong forward scattering. Recall constraints on the array reflection symmetry were imposed for observing directional scattering. Here, 15.2 and 16.9 dBi for the first and second geometries, respectively, are predicted numerically.

Multipole expansion is a useful tool to analyze scattering. However, multipoles themselves are not true eigenmodes of the structure. It is worth noting that one-to-one correspondence between eigenmodes and spherical multiples exists in structures obeying a rotational symmetry. In other cases, including those considered here, the far-field of a leaking mode can have several multipole contributions and vice versa. An eigenmode analysis of the wire bundles was performed numerically with CST. Quite a few modes have been found, and the results appear in Fig. 2(e) and (f), where resonance frequencies and Q-factors are summarized. There are many modes bunched around the peak. There are also several

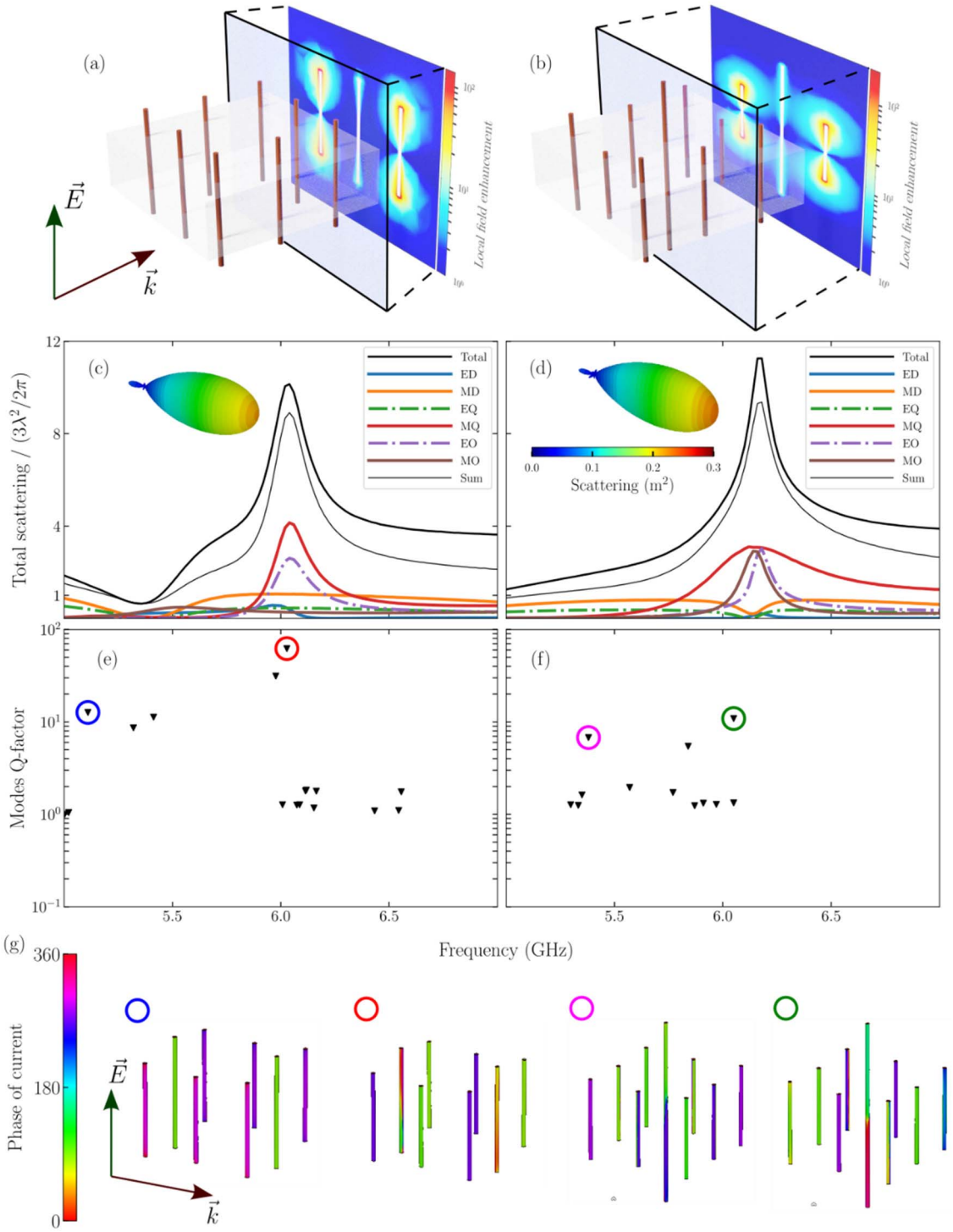

Fig. 2. Numerical analysis of wire bundles. (a) and (b) Schematics of the representative layouts. Incident field polarization and k-vector are depicted in (a). Scattered field intensities at the cut plane, crossing (b) structure's center and (a) back face, appear as color maps. The incident field amplitude is 1 V/m. (c) and (d) Scattering cross section, normalized to the dipole single-channel limit $[3\lambda^2/(2\pi)]$, as a function of operational frequency. Results in (c) correspond to the geometry in (a), while (d) is related to (b). Multipole expansion, summation, and contributions of each multipole are defined in legends. Abbreviations appear in the main text. Insets: far-field directivity patterns. (e) and (f) Eigenmodes—resonant frequencies and corresponding Q-factors. (g) Currents' phases on the wires for four eigenmodes, marked with colored circles in (e) and (f).

resonances at frequencies aside from the peak without a significant contribution to scattering. Corresponding Q-factors are ranging between 10 and 100, which is reasonable for open resonators. Overcoming those numbers is quite challenging with real lossy materials and open boundaries of the structures. Four representative modes indicated with colored

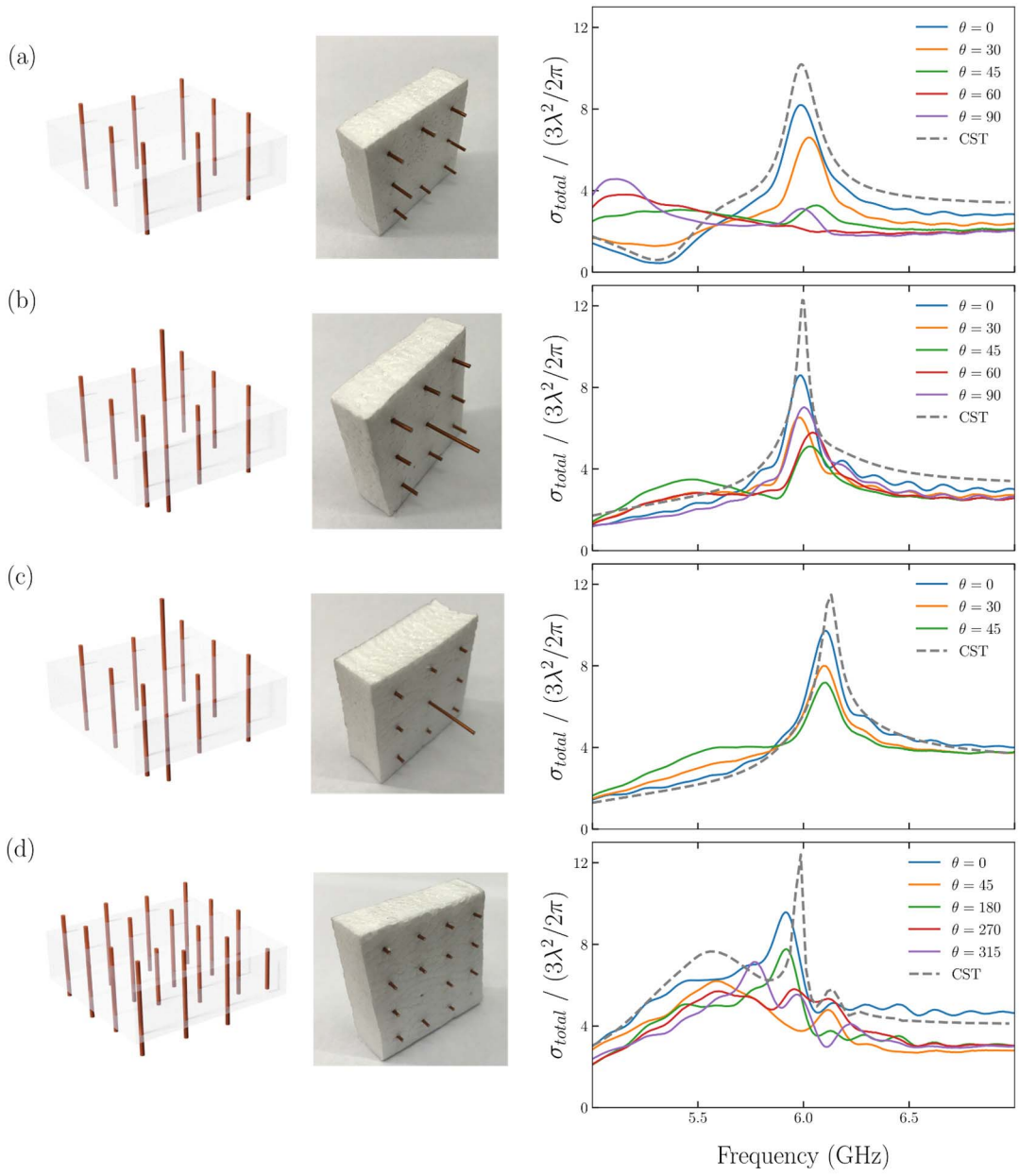

Fig. 3. Scattering cross-sectional spectra – simulation and experiment, for eight-element structure (a), 3×3 structures with $\pi/2$ (b), $\pi/4$ (c), and radial symmetry and 4×4 structure without radial symmetry (d). Black dashed line—numerical calculations and blue line ($\theta = 0°$) – normal incidence, for which the structures were designed. Different angles of incidence – curves are labeled in legends. Geometries – schematics and photographs of the samples appear to the left of the curves. Electrical field is polarized along the wires.

circles in Fig. 2(e) and (f) were picked up for further analysis. The corresponding current distributions associated with those modes appear in Fig. 2(g). Since the wire bundles scatter at higher-order multipole, the contributing eigenmodes also have a highly asymmetric phase structure.

IV. Experimental Demonstration

While only the two most promising geometries were comprehensively analyzed with the multipole expansion, the algorithm provides quite a few other solutions. Since superscatterers can be sensitive to fabrication imperfections, four geometries were chosen for experimental tests (Fig. 3). Geometrical details in matrix forms appear in the Supplementary Material. The copper wires with 0.5 mm radii were used for the samples manufacturing. An accuracy of relative wires' positioning and their lengths were checked with the caliper and are estimated to be better than ± 0.03 mm. The Styrofoam (white material on the photographs) is fully transparent for electromagnetic (EM) waves at 5–7 GHz. It is used as a host material to provide structural rigidity.

Two broadband horn antennas NATO IDPH-2018 (TX and RX—transmit and receive) were placed in front of each other at 2 m distance. Samples under the test were accurately located between the antennas. Electrical field polarization was aligned along the wires. Data acquisition was performed with Microwave Network Analyzer Keysight N5232b, and complex-valued transmission coefficients (S-parameters) were measured. The total scattering cross sections of the samples were obtained with the aid of optical theorem [9], [38]. Calibration of the system against a metal sphere allowed obtaining the absolute values of total scattering cross sections in m^2.

Scattering cross-sectional spectra are represented with blue solid lines in Fig. 3, while the corresponding numerical predictions appear as black dashed lines (all the panels). It is quite expected that the numerical data overestimate the experimental performances in such resonant structures. This is the manifestation of fabrication inaccuracies, which degrade constructive interference of several resonant multipoles. Nevertheless, it is quite remarkable that several of the considered geometries demonstrate only 10% difference between the predicted and observed peak values. The ratio between absorption and scattering cross sections was found to be around 2%, indicating the advantage of the chosen material platform.

While the structures were designed to demonstrate optimized performances only for a predefined angle of incidence ($\theta = 0°$), it is instructive to observe structures' behavior under tilted incidences (in all cases, the field is polarized along the wires). Several additional angles indicated in the legends (Fig. 3) were tested, and the experimental spectra appear as color lines in the plots. The behavior of all four geometries is diverse, underlining different operation principles. For example, geometries in the second and third lines [Fig. 3(b) and (c)] are almost immune to rotations, while the first structure is rather sensitive. The last structure contains a larger array (4×4) and demonstrates a much more complex modal hierarchy, resulting in a quite stochastic interference behavior.

V. Directivity Bounds

The beforehand considered structures, being constrained to have a strong forward scattering, will be assessed now in terms of directivities. Here, Chu–Harrington [39], [40] and Geyi [41] limits will be used as an assessment criterion. The diagram in Fig. 4 demonstrates directivities as a function of the normalized structure's size. R is a minimal radius of a sphere enclosing the object, while λ is the operational wavelength. The challenge in the field of superdirectivity is moving to the upper-left corner as much as possible [42]. Circles in Fig. 4 demonstrate the experimental performances of the structures in Fig. 3. All the samples demonstrate superdirective performances overcoming the Chu–Harrington limit by several dBi. Geometry B demonstrates the best results, as it has more constructively interfering multipoles in comparison with structure A (Fig. 2).

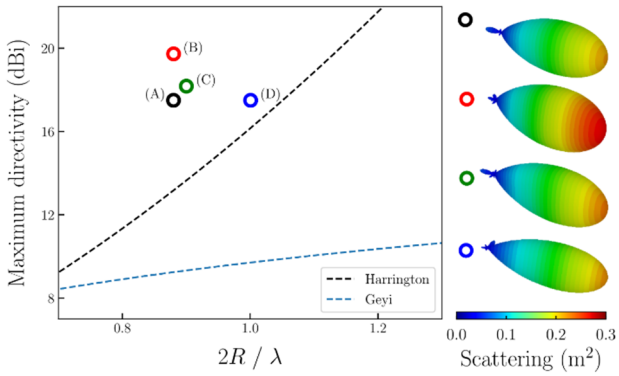

Fig. 4. Chu–Harrington and Geyi directivity bounds as a function of structure size, normalized to the wavelength. Colored circles are the directivities of the experimentally observed designs (Fig. 3). Directivity patterns appear in insets to the right.

VI. New Scattering Limit of Composite Structures

While 3×3 arrays were chosen to demonstrate superscattering performances (the reason will become evident hereinafter), bigger structures can be assessed. A comparison among 2×2, 3×3, 4×4, and 5×5 will be performed. Further increase in the array significantly enlarges the computation time and requires an extra layer of code optimization. Representative realizations of each size were selected and assessed with each other. Fig. 5 summarizes the geometries and the resulting cross sections. Each structure demonstrates superscattering performances, while the overall peak value starts saturating after 3×3, and further array enlargement does not grant a significant improvement [42]. Furthermore, increasing the number of wires in the bundle while keeping the geometrical support the same results in very dense packaging leading to instabilities.

After identifying this saturation effect empirically, further analysis can be done. In particular, the following observation can be made. A collection of N resonant dipoles, which are not coupled with each other, has a scattering cross section that is N times larger than the single-channel limit. Obviously, this uncoupled configuration is electrically large. The question is, can those dipoles, being placed within a dense array, where coupling effects take place and optimized for a maximized scattering cross section, demonstrate better performances with respect to the uncoupled case? This question has practical relevance in the field of radar deception, where folded foil dipoles (electromagnetic chaff) are used to screen a target. Is it better to deploy N uncoupled dipoles apart from an engineered structure? Fig. 5(b) demonstrates the scattering cross section normalized to the single-channel limit and to the number of wires within the array. It can be seen that only 2×2 and 3×3 arrays demonstrate values above 1. Any number above 1 shows that the engineered structure performs better than an uncoupled collection of dipoles. The 3×3 array demonstrates the best performance according to this new figure of merit—it is the reason why it was chosen for the detailed analysis at the very beginning.

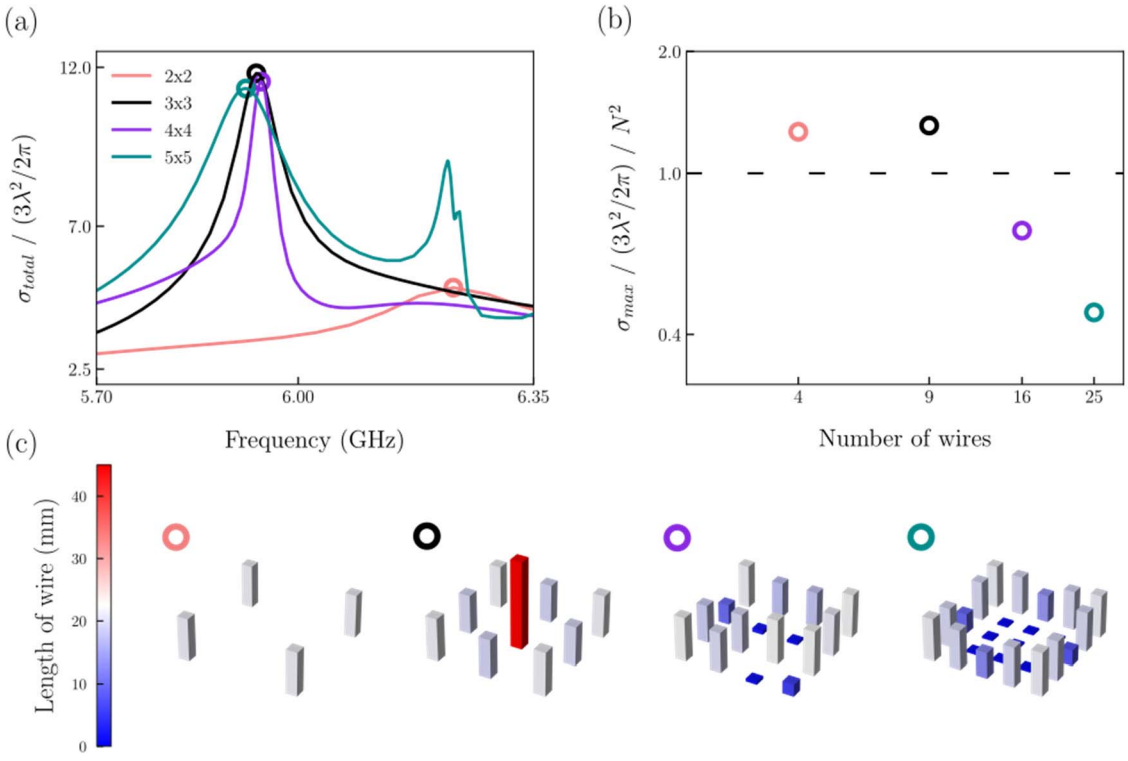

Fig. 5. (a) Scattering cross-sectional spectra normalized to the dipole single-channel limit $[3\lambda^2/(2\pi)]$ of four optimized designs with different array sizes (in legend), but with the same support. (b) Maximal scattering cross section normalized to the dipole single-channel limit and the number of wires with the array, as a function of the number of wires. (c) Lengths of wires in the considered structures.

VII. Conclusion

A genetic algorithm for scattering cross-sectional maximization was developed and applied to wire bundles. Isolated metal wires plugged within transparent host materials are among the best candidates for superscattering and superdirectivity applications. Capable of supporting high local fields, low-loss wire bundles can accommodate several resonant multipoles, constructively interfering to form the radiation pattern. Our designs demonstrate several geometries with three higher-order overlapping resonant multipoles, leading to more than one order of magnitude scattering cross-sectional enhancement with respect to the dipole single-channel limit. In terms of directivities, the genetically generated designs overcome Chu–Harrington and Geyi's limits by more than 8 dBi, demonstrating superdirective capabilities. The structures are designed to operate for a single polarization, i.e., along the wires. We also proposed a new scattering limit for assessing structures composed of near-field coupled resonators. If the value of total scattering cross section normalized to the single-channel limit and to the number of resonators within an array exceeds 1, then the coupling regime elevates the interaction. Otherwise, the coupling suppresses the total scattering of isolated resonators.

Genetically designed superscatterers with elevated performances can be used in a range of wireless applications, including point-to-point communications, smart beacons, and radar targets. For example, increasing visibility of an object, i.e., a small boat, interrogated with low-frequency over-the-horizon radars can be done with small foot-print superscatterers. Radar alignment marks for local navigation systems are another probable application.

References

[1] C. A. Balanis, *Antenna Theory: Analysis and Design*, 3rd ed. Hoboken, NJ, USA: Wiley, 2005.

[2] W. F. Bahret, "The beginnings of stealth tech nology," *IEEE Trans. Aerosp. Electron. Syst.*, vol. 29, no. 4, pp. 1377–1385, 1970.

[3] P.-Y. Chen, J. Soric, and A. Alù, "Invisibility and cloaking based on scattering cancellation," *Adv. Mater.*, vol. 24, no. 44, pp. OP281–OP304, Nov. 2012, doi: 10.1002/adma.201202624.

[4] V. Kozlov, D. Vovchuk, and P. Ginzburg, "Broadband radar invisibility with time-dependent metasurfaces," *Sci. Rep.*, vol. 11, no. 1, pp. 1–11, Jul. 2021, doi: 10.1038/s41598-021-93600-2.

[5] M. I. Skolnik, *Radar Handbook*, 3rd ed. New York, NY, USA: McGraw-Hill, 2008.

[6] C. F. Bohren and D. R. Huffman, *Absorption and Scattering of Light by Small Particles*. New York, NY, USA: Wiley, 1998, doi: 10.1002/9783527618156.

[7] R. F. Harrington, *Time-Harmonic Electromagnetic Fields*, 2nd ed. New York, NY, USA: Wiley, 2001.

[8] S. Krasikov *et al.*, "Multipolar engineering of subwavelength dielectric particles for scattering enhancement," *Phys. Rev. A, Gen. Phys.*, vol. 15, no. 2, Feb. 2021, Art. no. 024052, doi: 10.1103/PhysRevApplied.15.024052.

[9] D. Vovchuk, S. Kosulnikov, R. E. Noskov, and P. Ginzburg, "Wire resonator as a broadband Huygens superscatterer," *Phys. Rev. B, Condens. Matter*, vol. 102, no. 9, p. 94304, Sep. 2020, doi: 10.1103/PhysRevB.102.094304.

[10] R. C. Hansen, *Electrically Small, Superdirective, and Superconducting Antennas*. Hoboken, NJ, USA: Wiley, 2006.

[11] S. Kosulnikov, D. Filonov, A. Boag, and P. Ginzburg, "Volumetric metamaterials versus impedance surfaces in scattering applications," *Sci. Rep.*, vol. 11, no. 1, p. 9571, May 2021, doi: 10.1038/s41598-021-88421-2.

[12] D. W. Pearson, N. C. Steele, and R. F. Albrecht, *Artificial Neural Nets and Genetic Algorithms: Proceedings of the International Conference in*. Alès, France, 1995, doi: 10.1007/978-3-7091-7535-4.

[13] W. Vent, "Rechenberg, ingo, evolutionsstrategie—Optimierung technischer systeme nach prinzipien der biologischen Evolution. 170 S. mit 36 Abb. Frommann-Holzboog-Verlag. Stuttgart 1973. Broschiert," *Feddes Repertorium*, vol. 86, no. 5, p. 337, Sep. 1975, doi: 10.1002/fedr.4910860506.

[14] D. S. Linden and E. E. Altshuler, "Automating wire antenna design using genetic algorithms," *Microw. J.*, vol. 39, no. 3, pp. 74–81, 1996.

[15] C. Qian *et al.*, "Experimental observation of superscattering," *Phys. Rev. Lett.*, vol. 122, no. 6, p. 63901, Feb. 2019, doi: 10.1103/PhysRevLett.122.063901.

[16] K. Ladutenko, P. Belov, O. Peña-Rodríguez, A. Mirzaei, A. E. Miroshnichenko, and I. V. Shadrivov, "Superabsorption of light by nanoparticles," *Nanoscale*, vol. 7, no. 45, pp. 18897–18901, 2015, doi: 10.1039/c5nr05468k.

[17] A. Mirzaei, A. E. Miroshnichenko, I. V. Shadrivov, and Y. S. Kivshar, "Superscattering of light optimized by a genetic algorithm," *Appl. Phys. Lett.*, vol. 105, no. 1, Jul. 2014, Art. no. 011109, doi: 10.1063/1.4887475.

[18] Z. Ruan and S. Fan, "Design of subwavelength superscattering nanospheres," *Appl. Phys. Lett.*, vol. 98, no. 4, pp. 96–99, 2011, doi: 10.1063/1.3536475.

[19] J. Yelk, M. Sukharev, and T. Seideman, "Optimal design of nanoplasmonic materials using genetic algorithms as a multiparameter optimization tool," *J. Chem. Phys.*, vol. 129, no. 6, Aug. 2008, Art. no. 064706, doi: 10.1063/1.2961011.

[20] S. Arslanagić and R. W. Ziolkowski, "Highly subwavelength, superdirective cylindrical nanoantenna," *Phys. Rev. Lett.*, vol. 120, no. 23, Jun. 2018, Art. no. 237401, doi: 10.1103/PhysRevLett.120.237401.

[21] N. Bonod, S. Bidault, G. W. Burr, and M. Mivelle, "Evolutionary optimization of all-dielectric magnetic nanoantennas," *Adv. Opt. Mater.*, vol. 7, no. 10, May 2019, Art. no. 1900121, doi: 10.1002/adom.201900121.

[22] T. Feichtner, O. Selig, and B. Hecht, "Plasmonic nanoantenna design and fabrication based on evolutionary optimization," *Opt. Exp.*, vol. 25, no. 10, May 2017, Art. no. 10828, doi: 10.1364/oe.25.010828.

[23] T. Feichtner, O. Selig, M. Kiunke, and B. Hecht, "Evolutionary optimization of optical antennas," *Phys. Rev. Lett.*, vol. 109, no. 12, Sep. 2012, Art. no. 127701, doi: 10.1103/PhysRevLett.109.127701.

[24] P. I. Lazaridis *et al.*, "Comparison of evolutionary algorithms for LPDA antenna optimization," *Radio Sci.*, vol. 51, no. 8, pp. 1377–1384, Aug. 2016, doi: 10.1002/2015RS005913.

[25] S. Preble, M. Lipson, and H. Lipson, "Two-dimensional photonic crystals designed by evolutionary algorithms," *Appl. Phys. Lett.*, vol. 86, no. 6, Feb. 2005, Art. no. 061111, doi: 10.1063/1.1862783.

[26] P. Bennet *et al.*, "Analysis and fabrication of antireflective coating for photovoltaics based on a photonic-crystal concept and generated by evolutionary optimization," *Phys. Rev. B, Condens. Matter*, vol. 103, no. 12, Mar. 2021, Art. no. 125135, doi: 10.1103/PhysRevB.103.125135.

[27] P. Ginzburg, N. Berkovitch, A. Nevet, I. Shor, and M. Orenstein, "Resonances on-demand for plasmonic nano-particles," *Nano Lett.*, vol. 11, no. 6, pp. 2329–2333, 2011.

[28] P. Ginzburg, I. Shor, A. Nevet, N. Berkovitch, and M. Orenstein, "Plasmonic particles with engineered resonances-superfilters and superabsorbers," in *Proc. Quantum Electron. Laser Sci. Conf.*, Baltimore, MD, USA, May 2011, pp. 1–6.

[29] B. Balasubramanian *et al.*, "Magnetism of new metastable cobalt-nitride compounds," *Nanoscale*, vol. 10, no. 27, pp. 13011–13021, 2018, doi: 10.1039/c8nr02105h.

[30] T. L. Marzetta, "Super-directive antenna arrays: Fundamentals and new perspectives," in *Proc. 53rd Asilomar Conf. Signals, Syst., Comput.*, Nov. 2019, pp. 1–4, doi: 10.1109/IEEECONF44664.2019.9048753.

[31] W. K. Kahn, "A general characterization of superdirectivity," in *Proc. 1st URSI Atlantic Radio Sci. Conf. (URSI AT-RASC)*, May 2015, p. 1, doi: 10.1109/URSI-AT-RASC.2015.7302871.

[32] J. Yan *et al.*, "A method for optimising superdirectivity of coupled meta-atoms via planar directivity evaluation," *IEEE Open J. Antennas Propag.*, vol. 1, pp. 300–308, 2020, doi: 10.1109/OJAP.2020.3001579.

[33] V. Vulfin and R. Shavit, "Superscattering in 2D cylindrical structures," in *Proc. IEEE Antennas Propag. Soc. Int. Symp. (APSURSI)*, Sep. 2014, pp. 1439–1440, doi: 10.1109/APS.2014.6905045.

[34] S. J. Orfanidis, *Electromagnetic Waves and Antennas*. New Brunswick, NJ, USA: Rutgers Univ., 2016.

[35] V. Kozlov, S. Kosulnikov, D. Vovchuk, and P. Ginzburg, "Memory effects in scattering from accelerating bodies," *Adv. Photon.*, vol. 2, no. 5, Sep. 2020, Art. no. 056003, doi: 10.1117/1.AP.2.5.056003.

[36] V. Kozlov, D. Filonov, Y. Yankelevich, and P. Ginzburg, "Micro-Doppler frequency comb generation by rotating wire scatterers," *J. Quant. Spectrosc. Radiat. Transf.*, vol. 190, pp. 7–12, Mar. 2017, doi: 10.1016/j.jqsrt.2016.12.029.

[37] S. Ghosh, S. Das, S. Roy, S. K. M. Islam, and P. N. Suganthan, "A differential covariance matrix adaptation evolutionary algorithm for real parameter optimization," *Inf. Sci.*, vol. 182, no. 1, pp. 199–219, Jan. 2012, doi: 10.1016/j.ins.2011.08.014.

[38] R. G. Newton, "Optical theorem and beyond," *Amer. J. Phys.*, vol. 44, no. 7, p. 639, Jun. 1998, doi: 10.1119/1.10324.

[39] L. J. Chu, "Physical limitations of omni-directional antennas," *J. Appl. Phys.*, vol. 19, no. 12, pp. 1163–1175, Dec. 1948, doi: 10.1063/1.1715038.

[40] R. F. Harrington, "On the gain and beamwidth of directional antennas," *IEEE Trans. Antennas Propag.*, vol. AP-6, no. 3, pp. 219–225, Jul. 1958, doi: 10.1109/TAP.1958.1144605.

[41] W. Geyi, "Physical limitations of antenna," *IEEE Trans. Antennas Propag.*, vol. 51, no. 8, pp. 2116–2123, Aug. 2003, doi: 10.1109/TAP.2003.814754.

[42] M. Pigeon, C. Delaveaud, L. Rudant, and K. Belmkaddem, "Miniature directive antennas," *Int. J. Microw. Wireless Technol.*, vol. 6, no. 1, pp. 45–50, Feb. 2014, doi: 10.1017/S1759078713001098.

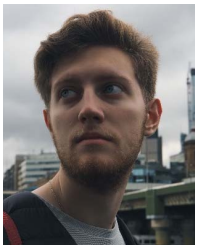

Konstantin Grotov is currently pursuing the bachelor's degree with ITMO University, Saint Petersburg, Russia.

His research interests include optimization methods, data science, and machine learning.

Dmytro Vovchuk received the B.Sc. and M.Sc. degrees from Yuriy Fedkovych Chernivtsi National University, Chernivtsi, Ukraine.

He has been performing his research with the School of Electrical Engineering, Tel Aviv University, Tel Aviv, Israel, since 2019. His research interests include radars, superscattering and superdirectivity, micro-Doppler, and deterministic chaos for communication systems.

Sergei Kosulnikov received the B.Sc. and M.Sc. degrees from ITMO University, Saint Petersburg, Russia, in 2011 and 2013, respectively.

In 2017, he defended a doctoral dissertation with the Department of Electronics and Nanoengineering, Aalto University, Espoo, Finland. He is currently a Post-Doctoral Research Fellow with the Dynamics of Nanostructures Laboratory, Tel Aviv University, Tel Aviv, Israel, where he is involved in engineering of superscattering and superdirectivity from miniaturized complex EM media structures.

Illya Gorbenko (Student Member, IEEE) is currently pursuing the M.Sc. degree in physics with ITMO University, Saint Petersburg, Russia.

He is a Junior Researcher with the Ioffe Institute, Saint Petersburg. His research interests include nonlinear plasmonics, plasma crystals, nanostructures, THz devices, and antennas.

Leon Shaposhnikov is currently pursuing the B.S. degree in theoretical physics with the School of Physics and Engineering, ITMO University, Saint Petersburg, Russia.

His research interests include topological photonics, metamaterials, and their applications.

Konstantin Ladutenko received the Ph.D. degree from ITMO University, Saint Petersburg, Russia, in 2017.

He is currently an Assistant Professor with ITMO University. His research interests include the areas of numerical methods and simulation in physics, with a focus on Mie theory and stochastic optimization.

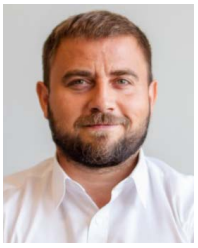

Pavel Belov (Member, IEEE) was born in 1977 in Ust-Ilimsk, Russia. He received the Ph.D. degree (Hons.) from ITMO University, Saint Petersburg, Russia, in 2000, and the D.Sc. degree in 2010. His Ph.D. theses was on the analytical modeling of electromagnetic crystals and the analytical modeling of metamaterials and new principle of sub-wavelength imaging. His D.Sc. thesis was on analytical modeling of electromagnetic crystals and left-handed materials.

He defended his Ph.D. thesis twice from ITMO University in 2003 and the Helsinki University of Technology, Espoo, Finland, in 2006. He was with Nokia, Espoo, Samsung Electronics, Suwon-si, South Korea, and Bosch, Uxbridge, U.K. He is currently a Russian Physicist and the Head of the International Research Centre for Nanophotonics and Metamaterials, Saint Petersburg, and the Physics and Engineering School. He has authored or coauthored more than 260 scientific articles in refereed journals, 300 conference proceedings, and 18 book chapters. His H-index is 57 (according Scopus). His work has generated over 11 000 citations.

Dr. Belov is a member of the council of young scientists and specialists of ITMO University. He is also a member of AP-S, ED-S, MTT-S, Laser and Electro-Optics Society (LEO-S), URSI, and SPIE scientific societies. He is a Laureate of the Russian Federation President's Prize in Science and Innovation for Young Scientists in 2009 (Presidential Decree No.139 of February 4, 2010). The prize is awarded for outstanding contributions to the physics of metamaterials and the development of devices for transmission and processing of super-resolution images.

Pavel Ginzburg (Member, IEEE) received the Ph.D. degree from Technion, Haifa, Israel, in 2011.

He is currently an Associated Professor with Tel Aviv University, Tel Aviv, Israel. He is also the Head of the Dynamics of Nanostructures Laboratory, encompassing theoretical group, optical spectroscopy, and radio waves labs. The laboratory runs multidisciplinary research in the field of bio-photonics quantum mechanics, nano-plasmonics, metamaterials, optical forces, and radio physics.

Dr. Ginzburg is a former EPSRC Research Fellow, an International Newton Research Fellow, and a Rothschild Fellow at King's College London.